Intercritical annealing of a PH 13-8 Mo maraging steel

Andreas Rosenauer1, Dominik Brandl2, Gerald Ressel2, Manfred Stadler3, Martin Stockinger4
and Ronald Schnitzer1

1Department of Materials Science, Montanuniversität Leoben, Franz-Josef-Straße 18, 8700 Leoben, Austria
2Materials Center Leoben Forschung GmbH, Roseggerstraße 12, 8700 Leoben, Austria
[3]voestalpine BÖHLER Edelstahl GmbH & Co KG, Mariazellerstraße 25, 8605 Kapfenberg, Austria
[4]Department Product Engineering, Montanuniversität Leoben, Franz-Josef-Straße 18, 8700 Leoben, Austria

Improved toughness properties of maraging steels can be achieved by overaging, i.e. performing the aging treatment at increased temperatures or with prolonged dwell times to increase the phase fraction of reverted austenite. However, in this case the toughness increase is accompanied by a considerable loss in hardness and strength. Hereby, the addition of intercritical annealing after solution annealing and prior to aging is assessed for a PH 13-8 Mo maraging steel. An in-depth microstructural characterization by means of transmission electron microscopy and atom probe tomography revealed that martensite becomes locally enriched in Ni after intercritical annealing. The inhomogeneous distribution of Ni within martensite leads to a promoted formation of reverted austenite during subsequent aging at moderate temperatures, meaning that compared to overaging, no excessive coarsening and dissolution of the β-NiAl precipitates takes place. The mechanical properties from tensile testing, Charpy V-notch impact testing and fracture toughness determination underpin an improvement in toughness while maintaining high hardness and strength. Ultimately, it is demonstrated that by implementing the presented heat treatment strategy, a remarkable combination of toughness and strength can be achieved for structural aircraft components where PH 13-8 Mo maraging steels are extensively used.

Keywords: *maraging steels, intercritical annealing, toughness improvement, transmission electron microscopy, atom probe tomography*

1. Introduction

The standard heat treatment of PH 13-8 Mo maraging steels, which are used for structural components in the aerospace industry, consists of solution annealing and subsequent aging. During the latter heat treatment step, reverted austenite (RA) and intermetallic β-NiAl precipitates are formed, which govern the mechanical properties of these alloys [1, 2].

In order to achieve high toughness, PH 13-8 Mo maraging steels are subjected to overaging, i.e. aging at increased temperatures or with prolonged dwell times. The improved toughness properties are mainly related to the increased phase fraction of RA. Nevertheless, overaging does also result in notably lower hardness and strength, which is particularly caused by excessive coarsening of the intermetallic precipitates [3]. An alternative approach to improve the toughness of PH 13-8 Mo maraging steels is implementing an intercritical annealing step, i.e. annealing in the dual-phase field of martensite and austenite, prior to aging [4, 5]. It was found that intercritical annealing results in local Ni enrichments in martensite, which promote the formation of RA during subsequent aging at moderate temperatures [5]. Due to the lower aging temperature compared to overaging, excessive coarsening of the precipitates is effectively suppressed.

The aim of this study is to elaborate on the microstructural evolution during intercritical annealing and subsequent aging of a PH 13-8 Mo maraging steel. In addition, specimens subjected to this adapted heat treatment are compared to overaged specimens, since both heat treatments lead to high phase fractions of RA. The comparison includes mechanical properties from tensile testing, Charpy V-notch impact testing and fracture toughness determination.

2. Experiment

2.1 Heat treatment and characterization of the microstructure

The investigated PH 13-8 Mo maraging steel was melted in a vacuum induction melting furnace and underwent vacuum arc remelting. Afterward, the ingot was hot rolled into round bars with 90 mm in diameter. The chemical composition is given in Table 1.

Table 1 Chemical composition of the investigated PH 13-8 Mo maraging steel (in wt.%)

C	N	Mn	Si	Cr	Mo	Ni	Al	Fe
0.03	0.01	0.10	0.10	12.8	2.3	8.0	1.1	Bal.

Cylindrical dilatometer specimens were machined from a round bar for a variation of heat treatments which was carried out in a TA Instruments DIL 805 A dilatometer. The heat treatment parameters are listed in Table 2.

Table 2 Conducted heat treatments in a dilatometer. For each annealing step, the heating rate was set to 1.5 K*s^{-1} and the cooling rate to -3.0 K*s^{-1}

Heat treatment	Solution annealing	Intercritical annealing	Aging
S+A	927°C / 0.5 h	-	552°C / 4 h
S+A$_{588°C}$	927°C / 0.5 h	-	588°C / 4 h
S+I	927°C / 0.5 h	700°C / 2 h	-
S+I+A	927°C / 0.5 h	760°C / 2 h	552°C / 4 h

Following metallographic preparation, each specimen was analyzed via X-ray diffraction (XRD) with a Bruker-AXS D8 ADVANCE diffractometer with Bragg-Brentano geometry in the 40-100° 2θ angular range.

The phase fractions of austenite were estimated from the diffractograms by using Rietveld refinement. In addition, the hardness of each specimen was determined by employing a Vickers indenter with 10 Kg load (HV10).

The specimen subjected to solution annealing and intercritical annealing at 700°C for 2 h without subsequent aging (S+I) underwent an in-depth microstructural characterization. Electrolytically polished samples were investigated with a ThermoFisher Scientific Talos F200X G2 transmission electron microscope (TEM) equipped with a Super-X EDS system. Furthermore, tips were prepared by focus ion beam (FIB) milling, which were afterward analyzed in a CAMECA IMAGO LEAP 3000X HR atom probe at 20 K in laser mode. For the atom probe tomography (APT) measurements, the laser energy was set to 0.2 nJ and the repetition rate to 200 kHz. Prior to the APT analysis, transmission Kikuchi diffraction (TKD) measurements were performed for gathering crystallographic information.

2.2 Mechanical testing

The same variation of heat treatments was carried out on samples for mechanical testing. Tensile testing with round specimens was performed at room temperature in accordance with the standard ASTM A370. For assessing the toughness after the different heat treatments, Charpy V-notch impact tests were performed at various temperatures. In addition, the fracture toughness (K_{IC}) at room temperature was determined according to the standard ASTM E399 for selected heat treatment conditions.

3. Results

Table 3 shows the phase fraction of austenite and the average Vickers hardness for the different heat treatments. The results show that in comparison to the standard heat treatment (S+A), the introduction of intercritical annealing (S+I+A) significantly increases the phase fraction of austenite (increase from 4.7 to 10.2 vol%). The highest phase fraction (14.2 vol%) was measured after overaging ($S+A_{588°C}$). However, due to the high aging temperature the hardness is considerably lower compared to the other heat treatment conditions. In contrast, the hardness after the S+I+A heat treatment is relatively high despite the high phase fraction of austenite.

Table 3 Phase fraction of austenite determined by XRD and average Vickers hardness for each heat treatment condition

Heat treatment	Phase fraction austenite [vol%]	Vickers hardness [HV10]
S+A	4.7 ± 1.0	446 ± 1
$S+A_{588°C}$	14.2 ± 2.8	384 ± 2
S+I	3.1 ± 0.5	331 ± 3
S+I+A	10.2 ± 2.2	434 ± 3

Figure 1 shows a bright field (BF) TEM image and the corresponding energy-dispersive X-ray spectroscopy (EDS) map for Ni of the microstructure after solution annealing and intercritical annealing at 700°C for 2 h (S+I). Dark elongated zones are visible in the EDS map. In these areas the Ni content is notably lower compared to the surrounding areas. The inhomogeneous distribution of substitutional atoms within this sample was investigated in more detail by APT. Figure 2 shows the distribution of Ni atoms in a tip which, according to the TKD measurement in advance, consisted entirely of martensite.

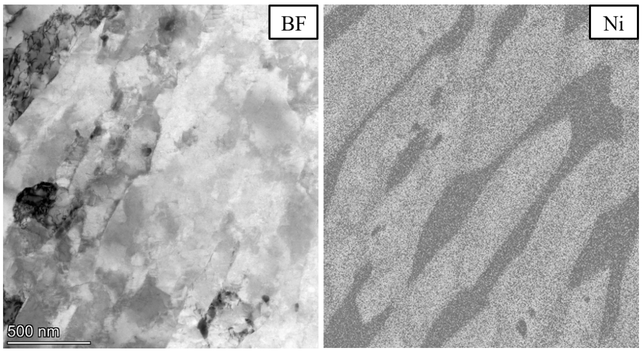

Figure 1 TEM image in BF mode and the corresponding EDS map for Ni after the S+I heat treatment

The lower part of the displayed tip exhibits a higher Ni content compared to the upper part. A cylindrical region of interest (ROI) is placed inside tip to measure the concentration profiles of Cr, Ni and Mo across these regions. The profiles quantitatively show that the Ni-enriched region is depleted in Cr and Mo and vice versa.

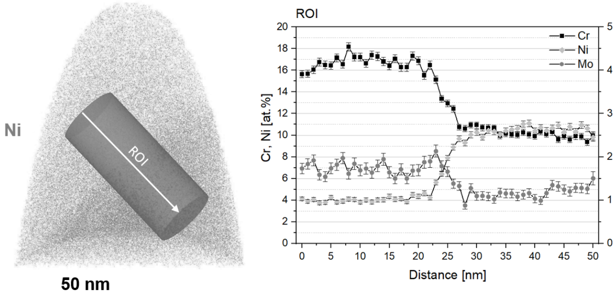

Figure 2 Distribution of Ni atoms for the analyzed APT tip and concentration profiles of Cr, Ni and Mo across the Ni-depleted and -enriched region

Figure 3 illustrates the results from the tensile tests at room temperature. The introduction of intercritical annealing at 760°C for 2 h (S+I+A) leads to a significantly higher yield and tensile strength compared to overaging ($S+A_{588°C}$). In comparison to the standard heat treatment (S+A), the strength is lower, but higher ductility was achieved. In the Charpy V-notch impact tests, the impact toughness was insignificantly improved through intercritical annealing. However, the fracture toughness K_{IC} was considerably increased from 96 to 149 MPa*m$^{0.5}$.

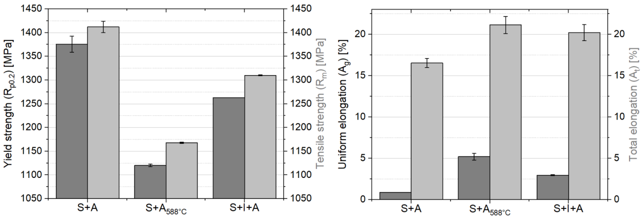

Figure 3 Results from the tensile tests at room temperature

4. Discussion

The inhomogeneous distribution of substitutional elements in martensite after intercritical annealing results from considerable partitioning of these atoms during this annealing step. Austenite becomes enriched in Ni during intercritical annealing, but depleted in Cr and Mo, and vice versa for martensite. The lower the intercritical annealing temperature, the lower the phase fraction of austenite and the more pronounced the Ni enrichment. As the TEM/EDS images in Figure 1 show Ni-enriched and -depleted zones in the microstructure, it is conceivable that the enriched regions were austenite grains during intercritical annealing. These regions transformed almost entirely into martensite during cooling, however, the Ni enrichment remained in the microstructure at room temperature. The Ni-depleted zones can be associated with regions that remained martensitic during intercritical annealing. The APT tip shown in Figure 2 contains both a Ni-enriched and -depleted zone and quantitatively underpin the inhomogeneous distribution of the substitutional elements in martensite after intercritical annealing.

It is postulated that the Ni enrichments in martensite are the root cause for the promoted formation of RA during subsequent aging. Therefore, it is possible to adjust high phase fractions of RA at moderate aging temperatures in PH 13-8 Mo maraging steels by implementing an intercritical annealing step prior to aging. Since lower intercritical annealing temperatures lead to more pronounced Ni enrichments in martensite, higher phase fractions of RA can be expected in such a case.

Even higher RA contents can be achieved by overaging. However, the drawback of this procedure are excessive coarsening and dissolution of the intermetallic β-NiAl precipitates, which provide the major strength contribution in maraging steels. Since intercritical annealing omits the necessity to perform aging at high temperatures or with prolonged dwell times in order to adjust high RA contents, significantly finer precipitates can be expected after the complete heat treatment. This is underpinned by the results from mechanical testing, since the hardness and strength was considerably higher after the S+I+A heat treatment compared to overaging ($S+A_{588°C}$). Due to the high phase fraction of RA, higher ductility and fracture toughness was measured in comparison to the standard heat treatment (S+A). Nevertheless, the impact energies from the Charpy V-notch impact test were insignificantly elevated by the addition of intercritical annealing, whereas overaging led to extraordinarily high impact energies. It is assumed that this is both due to the higher RA content and the softer martensitic matrix as the aging temperature was increased from 552 to 588°C in the $S+A_{588°C}$ heat treatment.

In summary, the results provide evidence that the addition of intercritical annealing in the heat treatment of PH 13-8 Mo maraging steels is a promising strategy to achieve a good combination of strength, ductility and fracture toughness. Improving the mechanical properties of theses alloys enable both more safety and lightweight design potential for structural aircraft components.

5. Conclusions

In this study, the influence of intercritical annealing on the microstructure and mechanical properties of a PH 13-8 Mo maraging steel was investigated. The following conclusions can be made:

1) Due to thorough partitioning during intercritical annealing, Ni-enriched regions are present in martensite at room temperature. These Ni enrichments promote to formation of RA during subsequent aging.

2) Since high phase fractions of RA can be adjusted at moderate aging temperature, excessive coarsening and dissolution of the intermetallic β-NiAl precipitates are prevented.

3) Higher hardness and strength can be achieved in comparison to overaging. Furthermore, the ductility and fracture toughness are higher compared to the standard heat treatment (S+A). However, no significant influence on the impact energies was registered, whereas high values were measured for the overaged samples, as the microstructure exhibits a higher RA content and a notably softer martensitic matrix.

4) The implementation of intercritical annealing enables to achieve a remarkable combination of high strength and good ductility and fracture toughness.

Acknowledgments

The authors gratefully acknowledge the financial support under the scope of the COMET program within the K2 Center “Integrated Computational Material, Process and Product Engineering (IC-MPPE)” (Project No 886385). This program is supported by the Austrian Federal Ministries for Climate Action, Environment, Energy, Mobility, Innovation and Technology (BMK) and for Digital and Economic Affairs (BMDW), represented by the Austrian Research Promotion Agency (FFG), and the federal states of Styria, Upper Austria and Tyrol.

References

1) V. Seetharamann: Mater. Sci. Eng. **47** (1981) 1-11.
2) R. Schnitzer, R. Radis, M. Nöhrer, M. Schober, R. Hochfellner, S. Zinner, E. Povoden-Karadeniz, E. Kozeschnik and H. Leitner: Mater. Chem. Phys. **112** (2010) 138-145.
3) P. W. Hochanadel, C. V. Robino, G. R. Edwards and M. J. Cieslak: Metall. Mater. Trans. A **25** (1994) 789-798.
4) Z. Guo, W. Sha, E. A. Wilson and R. W. Grey: ISIJ Int. **43** (2003) 1622-1629.
5) A. Rosenauer, D. Brandl, G. Ressel, S. Lukas, C. Gruber, M. Stockinger and R. Schnitzer: Adv. Eng. Mat. **25** (2023) 2300410.